



Prediction of dermal absorption from complex chemical mixtures: incorporation of vehicle effects and interactions into a QSPR framework

J. E. Riviere & J. D. Brooks

To cite this article: J. E. Riviere & J. D. Brooks (2007) Prediction of dermal absorption from complex chemical mixtures: incorporation of vehicle effects and interactions into a QSPR framework , SAR and QSAR in Environmental Research, 18:1-2, 31-44, DOI: [10.1080/10629360601033598](https://doi.org/10.1080/10629360601033598)

To link to this article: <https://doi.org/10.1080/10629360601033598>



Published online: 04 Dec 2010.



Submit your article to this journal [↗](#)



Article views: 172



Citing articles: 36 View citing articles [↗](#)

Prediction of dermal absorption from complex chemical mixtures: incorporation of vehicle effects and interactions into a QSPR framework†

J. E. RIVIERE* and J. D. BROOKS

Center for Chemical Toxicology Research and Pharmacokinetics, North Carolina State University, 4700 Hillsborough Street, Raleigh, NC 27606, USA

(Received 11 May 2006; in final form 27 August 2006)

Significant progress has been made on predicting dermal absorption/penetration of topically applied compounds by developing QSPR models based on linear free energy relations (LFER). However, all of these efforts have employed compounds applied to the skin in aqueous or single solvent systems, a dosing scenario that does not mimic occupational, environmental or pharmaceutical exposure. We have explored using hybrid QSPR equations describing individual compound penetration based on the molecular descriptors for the compound modified by a mixture factor (MF) which accounts for the physicochemical properties of the vehicle/mixture components. The MF is calculated based on percentage composition of the vehicle/mixture components and physical chemical properties selected using principal components analysis. This model has been applied to 12 different compounds in 24 mixtures for a total of 288 treatment combinations obtained from flow-through porcine skin diffusion cells and in an additional dataset of 10 of the same compounds in five mixtures for a total of 50 treatment combinations in the *ex vivo* isolated perfused porcine skin flap. The use of the MF in combination with a classic LFER based on penetrant properties significantly improved the ability to predict dermal absorption of compounds dosed in complex chemical mixtures.

Keywords: Dermal absorption; Chemical mixtures; QSAR; LFER

1. Introduction

It is axiomatic that for a topically applied compound to exert systemic toxicity, absorption across the dermal barrier is required. To be absorbed into the skin, a compound must first pass through the stratum corneum, continue through the epidermal layers and penetrate into the dermis where absorption into the dermal

*Corresponding author. Email: Jim_Riviere@ncsu.edu

†Presented at the 12th International Workshop on Quantitative Structure–Activity Relationships in Environmental Toxicology (QSAR2006), 8–12 May 2006, Lyon, France.

microcirculation becomes the portal for systemic exposure. If the compound has direct toxicity to the skin, systemic absorption is not required as the target cells could be any of those comprising the epidermis or dermis. Dermal absorption experiments generally involve experiments conducted using single compounds; hence the mechanisms of absorption of individual compounds have been extensively studied. Most risk-assessment profiles and mathematical models are based on the absorption kinetics of single compounds. A primary route of occupational and environmental exposure to toxic compounds is through the skin; however, such exposures are often to complex chemical mixtures. In fact, the effects of co-administered chemicals on the rate and extent of absorption of a topically applied systemic toxicant may determine whether toxicity is ever realised [1]. This dichotomy between the availability of data and absorption models based on single compounds with field exposure scenarios dominated by complex mixtures deserves further attention.

Significant progress has been made on predicting the dermal absorption and/or penetration of topically applied compounds across skin using QSPR models based on linear free energy relations (LFER) linking penetrant molecular descriptors to skin permeability (k_p) [2–4]. These efforts have employed compounds applied to the surface of skin in single solvent or aqueous systems. This exposure scenario does not reflect occupational, environmental nor pharmaceutical exposure where compounds are often exposed with associated solvents, contaminants or specific formulation additives. It is well known that such factors modulate absorption of compounds [5–7]. Chemical additives shown to modulate absorption include different solvents, surfactants, specific dermal penetration enhancers or other pharmaceutical additives that allow for cosmetic acceptability of the final formulation. Similarly, many occupational exposures are often associated with either waste chemicals or solvents and reactive agents used in manufacturing processes. Aqueous environmental exposures likewise include other contaminants associated with the compound of interest. Although it is known that such additives modulate absorption of compounds of interest, this has not been quantitatively addressed in the framework of QSPR models.

We have explored the use of hybrid QSPR equations describing individual compound penetration based on the molecular descriptors for the compound, modified by a mixture factor (MF) which accounts for the physicochemical properties of the vehicle/mixture components. The first study utilised an *in vitro* flow through porcine skin diffusion cell model [8]. The present contribution reviews this approach and extends it to a more complex vascularised model system, the isolated perfused porcine skin flap (IPPSF) that has previously been shown to be responsive to a number of absorption chemical modulators as well as being predictive of *in vivo* human absorption [9–11]. The original diffusion cell data [8] is included in the manuscript for comparison to the IPPSF results.

2. Model description

To demonstrate the usefulness of the mixture factor to predict absorption from complex chemical mixtures, we employed the Potts and Guy LFER model [4], the

Hostynek and Magee LFER model [12] and the Abraham and Martins LFER model [13] as our base equations, since they are representative of the dermal QSPR approaches presently available. Preliminary analyses applying 16 different LFER equations reviewed by Geinoz *et al.* [3] to our entire diffusion cell as well as IPPSF datasets demonstrated a superior fit of our data to the Abraham equation compared to most other models reviewed. It must be stressed that the purpose of this research is not to identify the optimal LFER for predicting dermal permeation, nor to validate that any of these models is predictive of dermal absorption. Instead, the focus is to determine if use of a mixture factor improves predictions. The models used are:

Potts and Guy [4]:

$$\log k_p = i + a \log P_{\text{oct}} + b \text{MW} \quad (1)$$

where k_p is the permeability coefficient for the diffusion cell experiments, P_{oct} is the octanol–water partition coefficient, and MW is the molecular weight of the permeant.

Hostynek and Magee [12]:

$$\log k_p = i + a \text{VEH} + b \text{MR} + c \text{HBA} + d \text{HBD} \quad (2)$$

where k_p is the permeability coefficient for the diffusion cell experiments, VEH is an indicator variable for the various vehicles, MR is the molar refractivity, HBA is the number of hydrogen bond acceptors and HBD is the number of hydrogen bond donors of the permeant.

Abraham and Martins [13]:

$$\log k_p = i + a \Sigma \alpha_2^{\text{H}} + b \Sigma \beta_2^{\text{H}} + s \pi_2^{\text{H}} + e R_2 + v V_x \quad (3)$$

where k_p is the permeability coefficient for the diffusion cell experiments, $\Sigma \alpha_2^{\text{H}}$ is the hydrogen-bond donor acidity, $\Sigma \beta_2^{\text{H}}$ is the hydrogen-bond acceptor basicity, π_2^{H} is the dipolarity/polarisability, R_2 represents the excess molar refractivity and V_x is the McGowan volume. For IPPSF experiments, perfusate flux $\log[\text{area under the curve}]$ (AUC) rather than $\log k_p$ was employed since it best represents total transdermal flux across this more complex, vascularised model system. Molecular descriptor values for these parameters were obtained from the literature; ChemOffice version 6.0.1 (CambridgeSoft.com, Cambridge, MA, USA); ClogP version 4.0 (BioByte.com Claremont, CA, USA); ADME Boxes version 2.2 (Pharma Algorithms, Inc., Toronto, Canada); SPARC online calculator (University of Georgia, Athens, GA, USA, <http://ibmlc2.chem.uga.edu/sparc>); Syracuse Research Corporation (Syracuse, NY, USA, <http://esc.syrres.com/interkow/physdemo.htm>); and logP.com (ChemSilico, Bedford, MA, USA, <http://www.logp.com>).

To incorporate mixture effects, another term is added called the mixture factor (MF) yielding:

Potts and Guy [4]:

$$\log k_p = i + m \text{MF} + a \log P_{\text{oct}} + b \text{MW}. \quad (4)$$

Table 1. Example calculation for methyl parathion (MP) in the water + SLS mixture in the IPPSF.

<i>Component</i>	μg	<i>Percentage</i>	<i>TPSA</i>	<i>Contribution</i>
Water	150,000	90.86	18.00	16.355
SLS	15,000	9.09	71.98	6.540
MP	87.9	0.053	118.42	0.063
			$\Sigma\text{TPSA} =$	22.958

Hostynek and Magee [12]:

$$\log k_p = i + m\text{MF} + a\text{VEH} + b\text{MR} + c\text{HBA} + d\text{HBD}. \quad (5)$$

Abraham and Martins [13]:

$$\log k_p = i + m\text{MF} + a\Sigma\alpha_2^{\text{H}} + b\Sigma\beta_2^{\text{H}} + s\pi_2^{\text{H}} + eR_2 + vV_x. \quad (6)$$

The parameters i , m , a , b , c , d , e , s and v are weighting coefficients coupling the molecular descriptors to skin permeability in the specific experimental system.

This concept allows an LFER equation to be defined across data collected from different mixtures. Hostynek and Magee [13] had used indicator variables embedded in LFER equations to allow analysis across exposures consisting of different vehicles or occlusive conditions. Unlike our approach, these indicator variables did not contain any information concerning the vehicles, but were a statistical regression tool to allow the base LFER model to be applied to penetrants dosed under different experimental conditions. The value for the MF is determined by examining the residual plot (actual *vs.* predicted $\log k_p$) generated from equations (4)–(6) based on molecular descriptors of the permeants as a function of the physical chemical properties of the mixture/solvents in which they were dosed. A number of available physical chemical properties of the mixture components were analysed, including parameters of molecular size and volume, hydrogen bonding, pKa, ovality, Henry's Law constant, polarizability, refractive indices, melting point, boiling point and vapour pressure. We then computed a composite physical chemical MF by weighting the component's physical chemical parameter (e.g. refractive index, etc.) by its contribution to its MF based on the summation of the weight percentage of each of the bulk components in the mixtures for a particular parameter. Table 1 shows the result of this calculation for methyl parathion (MP) in the water + SLS mixture in the IPPSF. TPSA is the topical polar surface area as calculated by ADME Boxes.

Minor mixture components based on weight percentages, in this case the actual penetrant, did not materially contribute to the value of the MF for a specific treatment and could be excluded. To confirm selection of these specific parameters, principal component analyses of these descriptors' effects on k_p also yielded three groups of descriptors which accounted for different patterns of variability seen. Full details of this approach have been presented elsewhere [8]. A similar process was employed for the IPPSF AUC data.

3. Materials and methods

Experimental techniques employed are fully described elsewhere: Porcine skin diffusion cells [1, 14, 15] and IPPSF [9]. Compounds used in these studies were radiolabelled (^{14}C) and perfusate flux determined using liquid scintillation counting. Compounds and mixtures studied are listed in tables 2–5. In both models, perfusate consisted of a

Table 2. Identity of 12 marker compounds investigated in *in vitro* diffusion cells.

<i>Substituted phenols</i>	<i>Organophosphates</i>	<i>Triazine herbicides</i>
Nonylphenol	Chlorpyrifos	Atrazine
Pentachlorophenol	Ethylparathion	Propazine
4-Nitrophenol	Methylparathion	Simazine
Phenol	Fenthion	Triazine

Table 3. Composition of 24 mixtures investigated in *in vitro* diffusion cells.

EtOH	PG
EtOH + MNA	PG + MNA
EtOH + SLS	PG + SLS
EtOH + MNA + SLS	PG + MNA + SLS
EtOH + water	PG + water
EtOH + water + MNA	PG + water + MNA
EtOH + water + SLS	PG + water + SLS
EtOH + water + MNA + SLS	PG + water + MNA + SLS
EtOH + PG	Water
EtOH + PG + MNA	Water + MNA
EtOH + PG + SLS	Water + SLS
EtOH + PG + MNA + SLS	Water + MNA + SLS

MNA = methylnicotinic acid; PG = propylene glycol (1,2-propanediol); SLS = sodium lauryl sulfate.

Table 4. Identity of 10 marker compounds investigated in IPPSF.

<i>Substituted phenols</i>	<i>Organophosphates</i>	<i>Triazine herbicides</i>
Nonylphenol	Chlorpyrifos	Atrazine
Pentachlorophenol	Ethylparathion	Propazine
4-Nitrophenol	Methylparathion	Simazine
		Triazine

Table 5. Composition of five mixtures investigated in the IPPSF.

EtOH
EtOH + water
Water
Water + SLS
PG

Pentachlorophenol was also investigated in EtOH + MNA ($n=3$), EtOH + water + MNA ($n=3$), PG + SLS ($n=3$) and water + PG ($n=3$); nonylphenol was not investigated in PG; triazine has not yet been investigated in water, water + SLS or PG. A total of 50 mixtures with 10 marker compounds were included in the analysis.

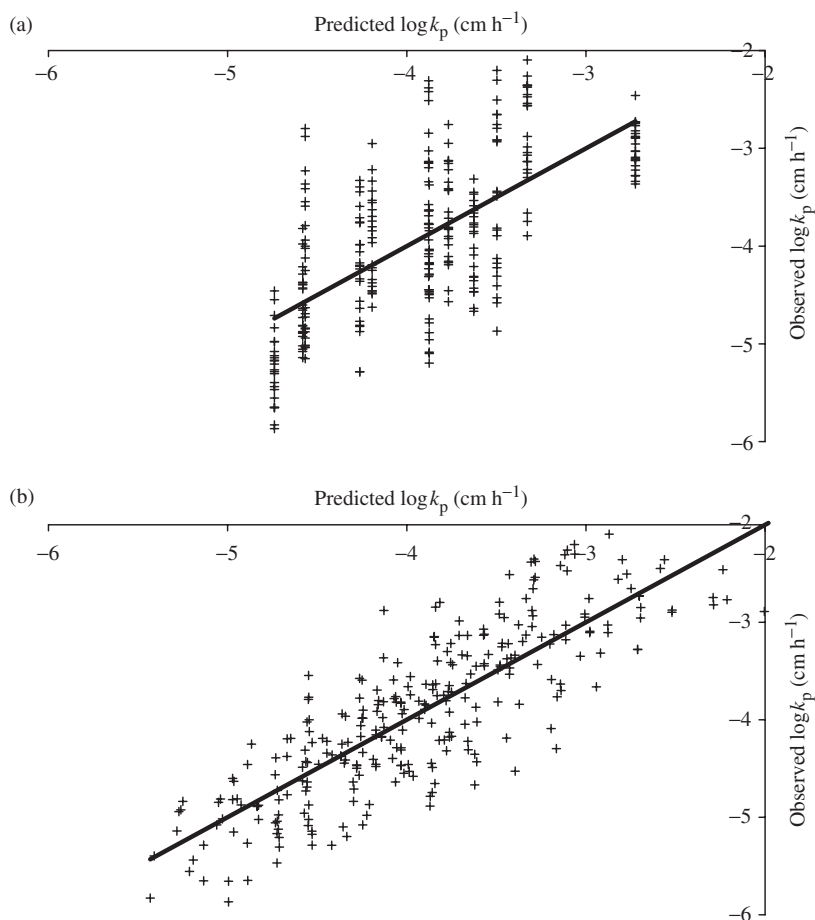


Figure 1. Predicted vs. observed $\log k_p$ of compound absorption in *in vitro* porcine skin diffusion cells, utilising the Potts and Guy model [4]. (a) No mixture factor. (b) Mixture factor equals topical polar surface area.

Krebs–Ringer bicarbonate buffer spiked with dextrose and bovine serum albumin. Skin was obtained from female weanling Yorkshire pigs. All compounds were dosed in equal volumes of topical mixtures. All experiments were conducted as a full factorial experimental design with $n = 4\text{--}5$ replicates per treatment. The permeability constant [k_p] (cm h^{-1}) of the compound through porcine skin was determined by dividing the steady state flux, calculated using regression as the slope of cumulative $\mu\text{g cm}^{-2}$ versus time regression, by applied surface concentration. AUC ($\%\text{D h mL}^{-1}$) was calculated using the trapezoidal rule, wherein the mean of the concentration of two adjacent time points was multiplied by the elapsed time of those two samples and added to the remaining means. Multiple regression analysis was carried out using SAS 9.1 for Windows (SAS Institute, Cary, NC).

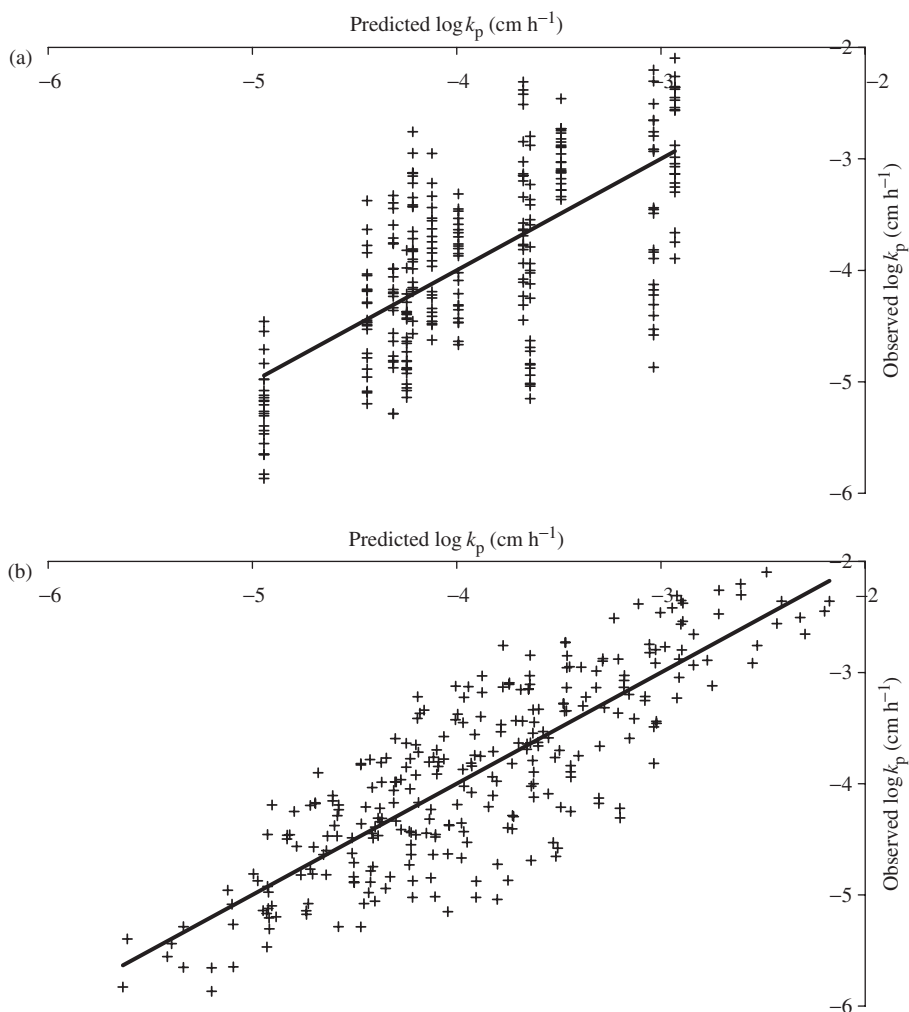


Figure 2. Predicted *vs.* observed $\log k_p$ of compound absorption in *in vitro* porcine skin diffusion cells, utilising the Hostynek and Magee model [12]. (a) No mixture factor. (b) Mixture factor equals topical polar surface area.

Tabulated statistics include the number of doses (n), the square of the correlation coefficients adjusted to the number of degrees of freedom (r^2), the cross-validation square of the correlation coefficients using the “leave-one-out” (q_{LOO}^2) and the “leave-a-random-25%-out” ($q_{25\%}^2$) techniques, the standard deviation (s) and the Fischer’s statistical test (F) for each equation.

We have used stepwise regression (SAS 9.1, Cary, NC, USA) with each model in addition to the two, three or five parameters established by the model authors, respectively, to determine the best MF for each equation. We report each model without and with the MFs.

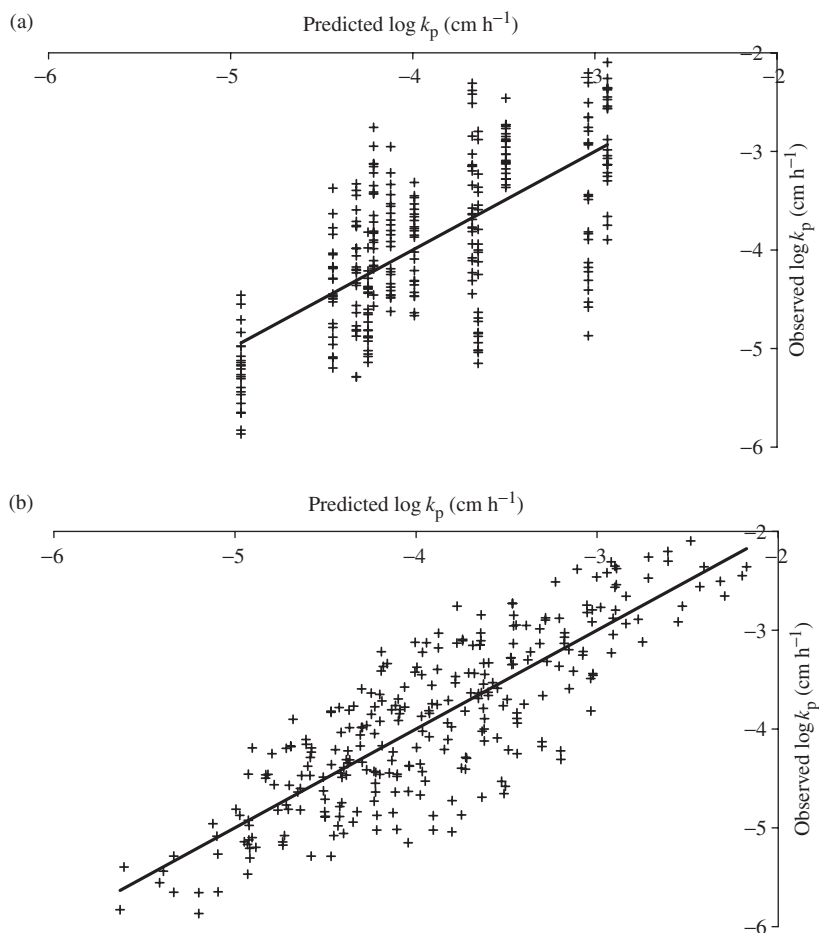


Figure 3. Predicted vs. observed $\log k_p$ of compound absorption in *in vitro* porcine skin diffusion cells, utilising the Abraham and Martins model [13]. (a) No mixture factor. (b) Mixture factor equals topical polar surface area.

4. Results and discussion

Figures 1(a), 2(a) and 3(a) depict the predicted versus observed permeability constants ($\log k_p$) for all 288 treatment combinations from the diffusion cell experiments without taking into account the specific mixtures in which these compounds were dosed. The LFER equations describing these data are listed in table 6 along with the statistical analysis of each equation. However, when vehicle/mixture component properties were then analysed, trends in residuals became evident which significantly improved predictability as judged by r^2 and tightness of prediction envelope. Figures 1(b), 2(b) and 3(b) illustrate this with MF being the topical polar surface area (TPSA) of the mixture components. The resulting LFER equations now including a mixture factor are

Table 6. LFER values for pig skin diffusion cells $\log k_p$ ($n = 288$).

r^2	q_{Loo}^2	$q_{25\%}^2$	s	F	i	m	MF	a	b	c			s	e	v
Potts and Guy [4]															
0.45	0.44	0.44	0.62	118	-2.81(0.13)	No MF		-0.30(0.03) * $\log P$	-0.00074(0.0007) * MW						
0.69	0.68	0.68	0.47	210	-2.05(0.11)	-0.04(0.003) * TPSA		-0.30(0.02) * $\log P$	-0.00080(0.0006) * MW						
0.67	0.66	0.66	0.48	193	-1.12(0.16)	-1.19(0.09) * #Accep.		-0.30(0.02) * $\log P$	-0.00081(0.0006) * MW						
Hostynek and Magee [12]															
0.45	0.44	0.44	0.62	78	-1.23(0.18)	No MF		-0.48(0.03) * MR	0.10(0.02) * HBA	-0.43(0.05) * HBD					
0.68	0.68	0.68	0.47	155	-0.49(0.15)	-0.04(0.003) * TPSA		-0.48(0.03) * MR	0.09(0.02) * HBA	-0.42(0.04) * HBD					
0.68	0.67	0.67	0.48	150	13.01(1.01)	-10.42(0.73) * Ref. Ind.		-0.49(0.03) * MR	0.10(0.02) * HBA	-0.45(0.04) * HBD					
Abraham and Martins [13]															
0.57	0.43	0.56	0.55	77	-0.19(0.27)	No MF		-1.49(0.31) * $\Sigma\alpha_2^H$	0.30(0.13) * $\Sigma\rho_2^H$	0.016(0.20) * π_2^H	-0.47(0.25) * R_2	-1.93(0.12) * V_x			
0.81	0.80	0.80	0.37	201	0.54(0.19)	-0.04(0.002) * TPSA		-1.45(0.21) * $\Sigma\alpha_2^H$	0.31(0.09) * $\Sigma\rho_2^H$	-0.004(0.13) * π_2^H	-0.45(0.17) * R_2	-1.92(0.08) * V_x			
0.80	0.79	0.79	0.37	192	13.98(0.81)	-10.38(0.58) * Ref. Ind.		-1.54(0.21) * $\Sigma\alpha_2^H$	0.25(0.09) * $\Sigma\rho_2^H$	0.092(0.13) * π_2^H	-0.53(0.17) * R_2	-1.92(0.08) * V_x			

Standard error in parentheses.

TPSA = topological polar surface area (calculated by ADME).

Accep. = number of hydrogen bond acceptors (calculated by log P .com).

Ref. Ind. = refractive index (calculated by SPARC).

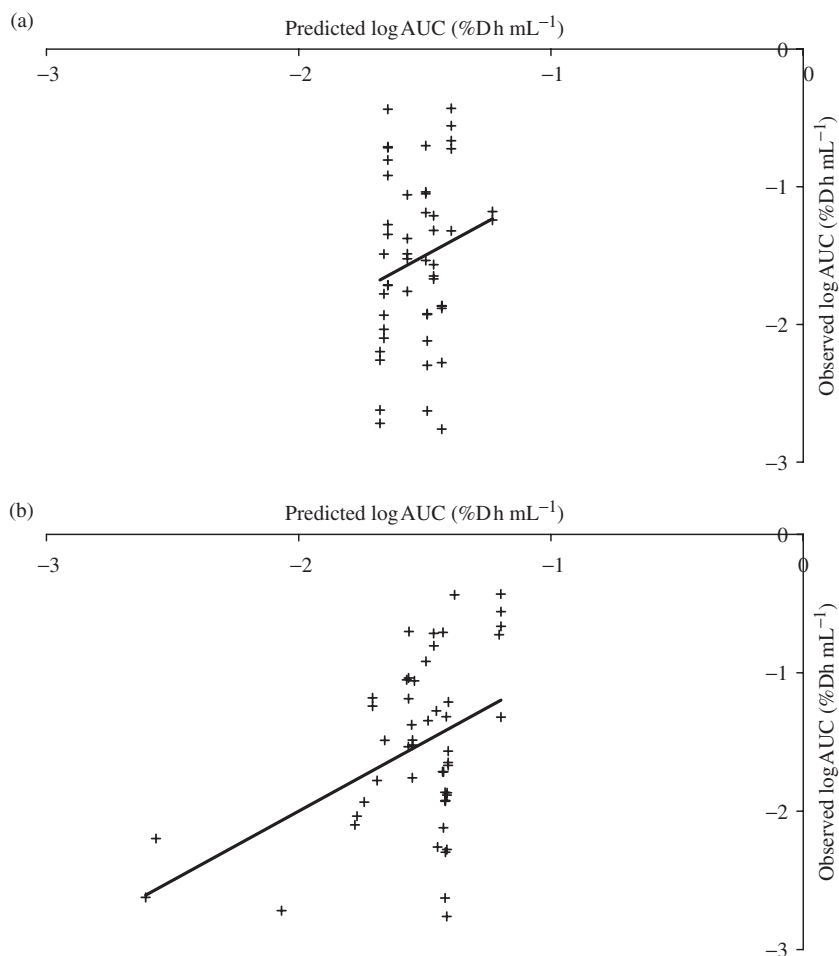


Figure 4. Predicted vs. observed log AUC of compound absorption in the IPPSF, utilising the Potts and Guy model [4]. (a) No mixture factor. (b) Mixture factor equals partition coefficient.

listed in table 6. We have listed two mixture factors in each case, for comparison purposes.

Figures 4(a), 5(a) and 6(a) depict the parallel analysis for log AUC from IPPSF studies in the absence of a MF. Figures 4(b), 5(b) and 6(b) depict the parallel analysis for log AUC from IPPSF studies with a MF. The LFER equations describing these data are listed in table 7 along with the statistical analysis of each equation.

As can be seen by comparing the (a) portion of each figure with the (b) portion, use of a MF significantly improved predictability of both $\log k_p$ and log AUC for diffusion cell and IPPSF data, respectively. The relative improvement in diffusion cell data was the greater, a finding not surprising since simpler biology and physical chemistry is involved in this model which lacks a viable dermis and vascular system. This is especially evident

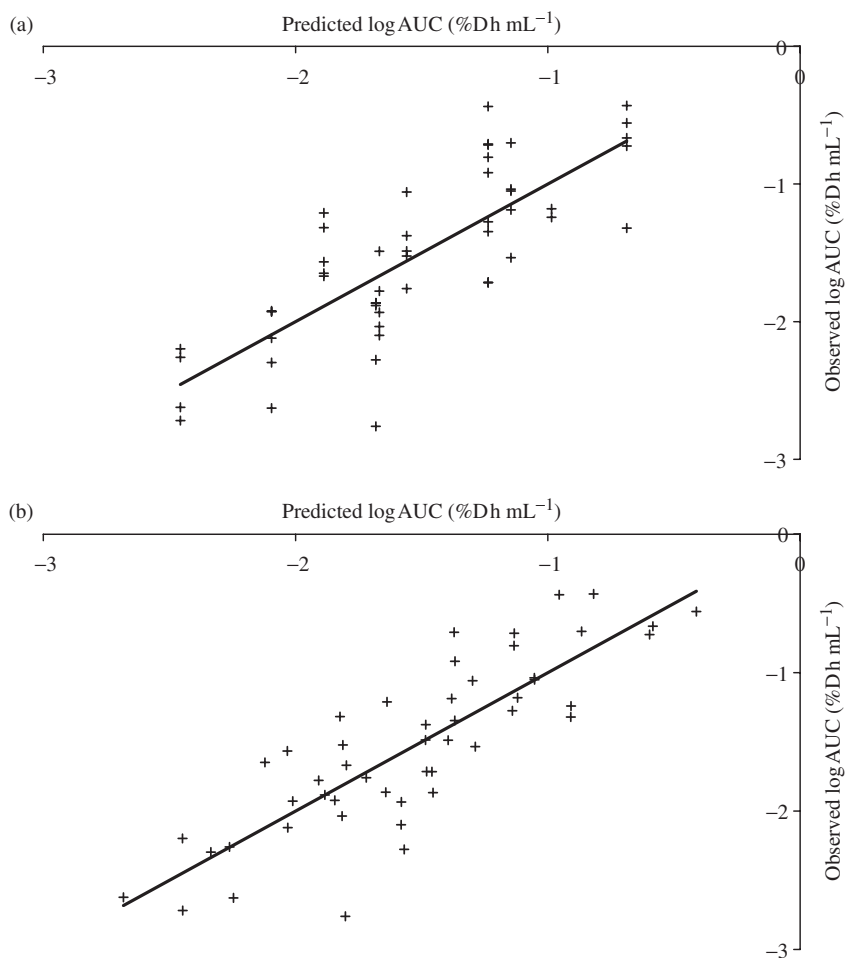


Figure 5. Predicted vs. observed log AUC of compound absorption in the IPPSF, utilising the Hostynek and Magee model [12]. (a) No mixture factor. (b) Mixture factor equals log water solubility.

in a comparison of the diffusion cell data with the IPPSF data while utilising the Potts and Guy model [4] in figures 1 and 4. This simple model lacks the robustness necessary to describe the more complex IPPSF system.

k_p cannot easily be calculated in the IPPSF. AUC is a secondary pharmacokinetic parameter and is not a primary physicochemical property of a molecule's interaction with skin. It is an aggregate parameter that reflects multiple interactions with the stratum corneum barrier, epidermis and dermis as well as vascular uptake by the intact vascular system of the IPPSF. We have previously defined IPPSF pharmacokinetic models that may generate parameters better suited to these types of analyses, in that they would reflect distinct skin uptake processes [16–18].

These analyses raise a number of issues. First, it must be assessed whether the molecular descriptors used to describe single compound LFER equations are optimal

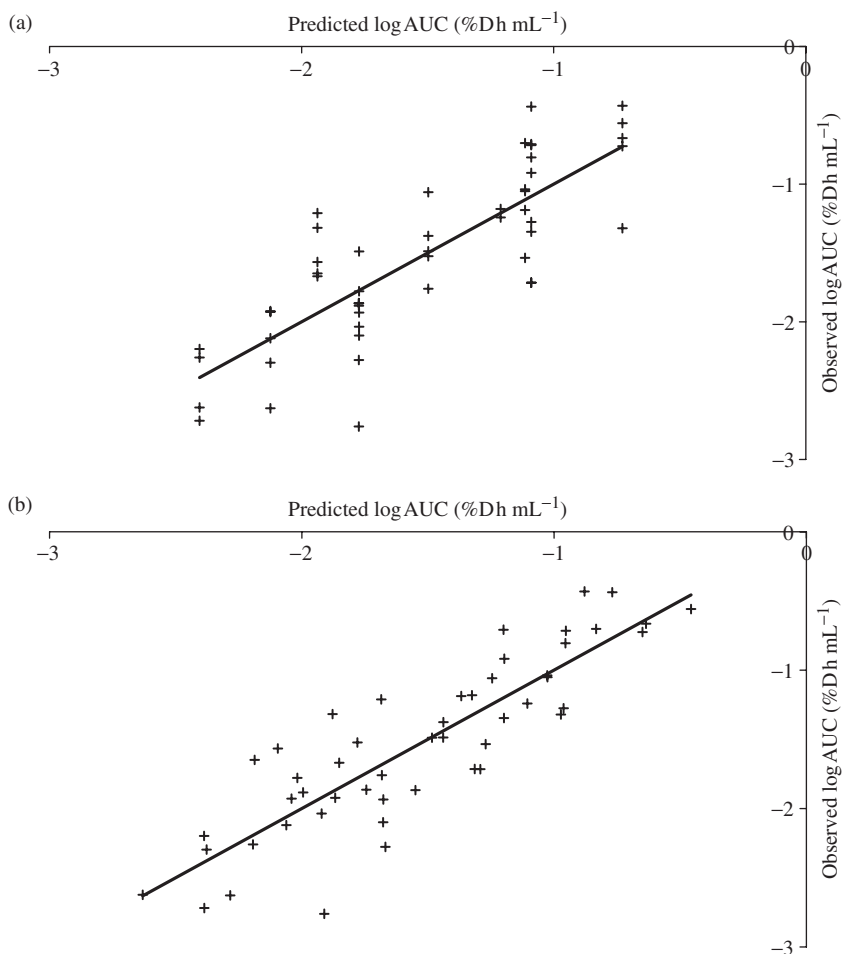


Figure 6. Predicted vs. observed log AUC of compound absorption in the IPPSF, utilising the Abraham and Martins model [13]. (a). No mixture factor. (b). Mixture factor equals log water solubility.

when a MF is included in the analysis. Second, the mixture factor selected may not be the optimal for all chemical mixtures. More work needs to be done to determine molecular descriptors optimal for specific penetrant–mixture combinations. Third, additional compounds and mixtures are presently being investigated to broaden the inference space (defined by both penetrant and mixture component physical chemical properties) over which these predictions would be expected to hold.

In conclusion, the improvement on the prediction of flow-through diffusion cell permeability across all treatments is clearly evident, independent of which base LFER is used. This clearly demonstrates the utility of a MF, and more generally the importance of taking into consideration both penetrant and mixture component properties. It must be stressed that any MF identified is not the final form of this analysis. The final form

Table 7. LFER values for IPPSF log AUC ($n=50$).

r^2	q_{Loo}^2	$q_{25\%}^2$	s	F	i	m	MF	a	b	c				s	e	v
Potts and Guy [4]																
-0.01	0.03	0.09	0.61	0.9	-1.23(0.39)	No MF		-0.07(0.07) * $\log P$	-0.0003(0.0020) * MW							
0.14	0.09	0.10	0.57	4	-0.91(0.38)		-0.0022(0.0007) * P_{oct}	0.14(0.10) * $\log P$	-0.0040(0.0023) * MW							
0.14	0.08	0.06	0.57	4	-1.86(0.42)		-1947(658) * $1/WS$	-0.08(0.07) * $\log P$	0.0033(0.0022) * MW							
Hostynek and Magee [12]																
0.60	0.57	0.57	0.39	26	1.09(0.35)	No MF		-0.45(0.06) * MR	0.09(0.03) * HBA							
0.68	0.65	0.65	0.35	27	0.65(0.34)		0.31(0.09) * $\log WS$	-0.47(0.05) * MR	0.10(0.03) * HBA							
0.68	0.65	0.65	0.35	27	5.00(1.16)		-3.52(1.01) * Ovality	-0.46(0.05) * MR	0.10(0.03) * HBA							
Abraham and Martins [13]																
0.63	0.59	0.59	0.37	18	1.48(0.66)	No MF		-2.22(0.60) * $\Sigma\alpha_2^H$	-0.75(0.20) * β_2^H	0.49(0.38) * π_2^H	-0.04(0.44) * R_2	-1.32(0.25) * V_x				
0.72	0.68	0.69	0.33	22	1.11(0.58)		0.32(0.08) * $\log WS$	-2.38(0.52) * $\Sigma\alpha_2^H$	-0.73(0.18) * $\Sigma\beta_2^H$	0.37(0.34) * π_2^H	0.15(0.38) * R_2	-1.42(0.22) * V_x				
0.72	0.68	0.68	0.33	22	5.64(1.24)		-3.63(0.95) * Ovality	-2.41(0.53) * $\Sigma\alpha_2^H$	-0.73(0.18) * $\Sigma\beta_2^H$	0.37(0.34) * π_2^H	0.14(0.38) * R_2	-1.42(0.22) * V_x				

Standard error in parentheses.

 P_{oct} = octanol-water partition coefficient (literature values in Syracuse Research database). $1/WS$ = inverse of the water solubility (literature values in Syracuse Research database). $\log WS$ = log water solubility (calculated by ADME).

Ovality (calculated by ChemOffice).

of such a modified mixture LFER must await further research. This includes defining which physical chemical property of the mixture best describes the mixture factor (MF). However, the finding that a MF can be used to extrapolate compound dermal absorption data across different vehicles and mixture combinations, in two biological systems using three different LFER models, is a significant finding which we believe would have impact on the occupational risk assessment process. It would allow single compound data collected in multiple research environments, and resulting single compound LFER determined in different studies to be modified based on mixture component or vehicle properties.

Acknowledgments

This work was supported by National Institute of Occupational Safety and Health grant NIOSH R01 OH 07555.

References

- [1] J.E. Riviere. *Dermal Absorption Models in Toxicology and Pharmacology*, Taylor and Francis, New York (2006).
- [2] M.H. Abraham, H.S. Chada, F. Martins, R.C. Mitchell, M.W. Bradbury, J.A. Gratton. *Pestic. Sci.*, **55**, 78 (1999).
- [3] S. Geinoz, R.H. Guy, B. Testa, P.A. Carrupt. *Pharm. Res.*, **21**, 83 (2004).
- [4] R.O. Potts, R.H. Guy. *Pharm. Res.*, **9**, 663 (1992).
- [5] J.D. Brooks, J.E. Riviere. *Fundam. Appl. Toxicol.*, **32**, 233 (1996).
- [6] J.E. Riviere, R.E. Baynes, J.D. Brooks, J.L. Yeatts, N.A. Monteiro-Riviere. *J. Toxicol. Environ. Health A*, **66**, 131 (2003).
- [7] C. Rosado, S.E. Cross, W.J. Pugh, M.S. Roberts, J. Hadgraft. *Pharm. Res.*, **20**, 1502 (2003).
- [8] J.E. Riviere, J.D. Brooks. *Toxicol. Appl. Pharmacol.*, **208**, 99 (2005).
- [9] J.E. Riviere, K.F. Bowman, N.A. Monteiro-Riviere, L.P. Dix, M.P. Carver. *Fundam. Appl. Toxicol.*, **7**, 444 (1986).
- [10] G.L. Qiao, J.D. Brooks, R.E. Baynes, N.A. Monteiro-Riviere, P.L. Williams, J.E. Riviere. *Toxicol. Appl. Pharmacol.*, **141**, 473 (1996).
- [11] R.C. Wester, J. Melendres, L. Sedik, H.I. Maibach, J.E. Riviere. *Toxicol. Appl. Pharmacol.*, **151**, 159 (1998).
- [12] L.J. Hostynek, P.S. Magee. *Quant. Struct. Act. Relat.*, **16**, 473 (1997).
- [13] M.H. Abraham, F. Martins. *J. Pharm. Sci.*, **93**, 1508 (2004).
- [14] R.L. Bronaugh, R.F. Stewart. *J. Pharm. Sci.*, **74**, 64 (1985).
- [15] S.K. Chang, J.E. Riviere. *Fundam. Appl. Toxicol.*, **17**, 494 (1991).
- [16] C.E. Smith, P.L. Williams, J.E. Riviere. 1995 *Proc. Biomet. Sec., Am. Stat. Assoc.*, pp. 449–454, American Statistical Association, Washington, DC (1996).
- [17] P.L. Williams, M.P. Carver, J.E. Riviere. *J. Pharm. Sci.*, **79**, 305 (1990).
- [18] J.E. Riviere, C.E. Smith, K. Budsaba, J.D. Brooks, E.J. Olajos, H. Salem, N.A. Monteiro-Riviere. *J. Appl. Toxicol.*, **21**, 91 (2001).